International Journal of Fracture, Vol 16, No. 4, August 1980

Alphen aan den Rijn, The Netherlands



# Compliance and stress intensity coefficients for short bar specimens with chevron notches*

D. MUNZ**, R.T. BUBSEY and J.E. SRAWLEY

*National Aeronautics and Space Administration, Lewis Research Center, Cleveland, Ohio* 44135, *USA*

(Received November 30, 1978)

ABSTRACT

For the determination of fracture toughness especially with brittle materials, a short bar specimen with rectangular cross section and chevron notch can be used. As the crack propagates from the tip of the triangular notch, the load increases to a maximum then decreases. To obtain the relation between the fracture toughness $K_{Ic}$ and maximum load $P_{max}$, calculations of Srawley and Gross for specimens with a straight-through crack were applied to the specimens with chevron notches. For the specimens with a straight-through crack, an analytical expression was obtained. This expression was used for the calculation of the $K_{Ic} - P_{max}$ relation under the assumption that the change of the compliance with crack length for the specimen with a chevron notch is the same as for a specimen with a straight-through crack.

Comparative compliance calibrations with specimens of different geometries agreed very closely with the analytical results for the $K_{Ic} - P_{max}$ relation. For the first part of crack extension before reaching maximum load, the dimensionless quantity $Y^* = K_{Ic}B\sqrt{W}/P$ where $B$ and $W$ are the specimen thickness and width, and $P$ the applied load, is greater for the analytical approach than that obtained from the experimental results. This difference can be explained by applying the slice model proposed by Bluhm.

## 1. Introduction

There exists no standard test for the determination of fracture toughness $K_{Ic}$ of brittle nonmetallic materials. Many types of specimens, such as the single edge notch bend specimen, the double torsion specimen, the double cantilever beam specimen, and the surface flawed specimen are currently used. These specimens have either blunt notches produced by saw cutting, or cracks produced by wedge loading or by local thermal shock. Specimens with blunt notches can overestimate $K_{Ic}$. Precracked specimens are difficult to prepare in a reproducible manner, and the initial crack front often cannot be seen on the fracture surface after testing, making it nearly impossible to measure the initial crack length. To overcome these difficulties Barker [1] has proposed a specimen with a chevron-notch, in which a crack originates at the tip of the triangular ligament during loading (Fig. 1).

Specimens with a chevron notch were first used by Nakajama [2] and later on by Tattersall and Tappin [3] in bend tests. For the chevron-notch specimen the necessary load for crack extension first increases to a maximum, and then decreases. Tattersall and Tappin determined the area under the load *vs.* deflection curve and divided it by the fracture area to obtain an average fracture surface energy. Barker used the maximum load for fracture toughness determination since for a given chevron-notch specimen

* Work done under NASA-DOE Interagency Agreement number EC-77-A-31-1040.

** National Research Council Senior Research Associate from German Aerospace Research Establishment (DFVLR), Cologne, FR Germany.

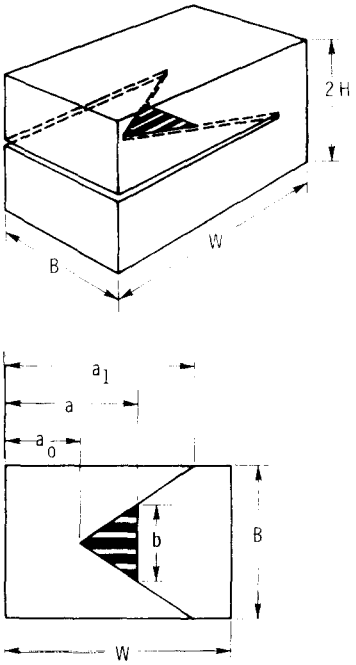


Figure 1. Short bar specimen.

geometry, the crack length at maximum load will be independent of the test material. This type of specimen has the advantage that a sharp crack is produced during loading, making it necessary only to measure the maximum load. The functional relation between the maximum load ($P_{max}$), the specimen geometry, and $K_{Ic}$, however, must be known. Barker used in his experiments a specimen with a circular cross section (short rod specimen) of fixed overall geometry, and obtained the relationship between $P_{max}$ and $K_{Ic}$ by comparing with materials of known $K_{Ic}$ values determined by standard methods. Recently Barker [4] also used a specimen with rectangular cross section (short bar specimen), designed in such a way that the same maximum load is obtained as for the short rod specimen. This specimen has been tested in a specially designed device, which applies a distributed load on the specimen arms.

For universal application of the short bar specimen, the relation between $K_{Ic}$, $P_{max}$ and the geometric variables has to be known. In this paper, calculations of Srawley and Gross [5] for a specimen with a straight-through crack are applied to the specimen with a chevron notch, and comparative results of compliance calibrations are presented. To explain the difference in compliance between the specimens with a straight-through crack and that with a chevron notch, the slice model of Bluhm [6, 7] is applied.

## 2. Stress intensity factor for a specimen with a straight-through crack

For a straight-through crack, the short bar specimen is similar to a double cantilever beam specimen but with a smaller width-to-height ($W/2H$) ratio. For a broad range of crack length-to-width ratios ($\alpha = a/W$) and $W/H$ ratios, the results of Srawley and Gross [5] can be used. To calculate the $Y$ function in the equation

$$K = \frac{P}{B\sqrt{W}} Y, \tag{1}$$

where $K$ is the stress intensity factor, $P$ the applied load and $B$ the thickness of the specimen, Srawley and Gross considered two extreme situations. For a specimen with ligament $(W-a)$ small compared to crack length $(a)$, they used a solution published by Paris and Sih [8] which can be written in the form

$$Y_1 = \frac{2.702 + 1.628\alpha}{(1-\alpha)^{3/2}} \tag{2}$$

For a specimen with a short crack length, the ligament size has no effect. For this ligament-independent type of specimen Gross and Srawley [9] found

$$Y_2 = \sqrt{12\frac{W^3}{H^3}}\left(\alpha + \frac{0.679}{W/H}\right) \tag{3}$$

Instead of the 0.679 of Eqn. (3), 0.7 is used in [5] and 0.688 in [9]. For the specimen geometry used here, however, the value of 0.679 is more accurate.

For a specimen with intermediate crack length the $Y$ function can be obtained by superposition of $Y_1$ and $Y_2$. First, two functions $F_1$ and $F_2$ are defined:

$$F_1 = \frac{Y_1(1-\alpha)^{3/2}}{\alpha} = \frac{2.702}{\alpha} + 1.628 \tag{4}$$

and

$$F_2 = \frac{Y_2(1-\alpha)^{3/2}}{\alpha} = \sqrt{12\frac{W^3}{H^3}(1-\alpha)^3}\left(1 + \frac{0.679}{\alpha(W/H)}\right). \tag{5}$$

An exponential superposition is used for $F_1$ and $F_2$:

$$e^F = e^{F_1} + e^{F_2}, \tag{6}$$

from which

$$F = \ln(\exp F_1 + \exp F_2), \tag{7}$$

and

$$Y = \frac{F \cdot \alpha}{(1-\alpha)^{3/2}}. \tag{8}$$

For $2 \leq W/H \leq 4$ and $0.2 \leq \alpha \leq 0.5$, calculations of $Y$ with Eqns. (4) to (8) agree with boundary collocation results of Srawley and Gross [5] within ±2.5%. New calculations of Gross [10] show even better agreement.

### 3. $P_{max} - K_{Ic}$ relation for the short bar specimen

As shown in Fig. 1, the geometry of the short bar specimen is defined by the thickness $B$, the width $W$, the height $2H$, and the crack length parameters $a_0$ and $a_1$. The crack extends under increasing load from $a_0$. At crack length $a$, crack front length is

$$b = B\frac{a-a_0}{a_1-a_0} = B\frac{\alpha-\alpha_0}{\alpha_1-\alpha_0} \tag{9}$$

The relation between $P_{max}$ and $K_{Ic}$ can be obtained using the energy approach of fracture mechanics. The available energy for extension of the crack by $\Delta a$ is given by

$$\Delta U = \frac{P^2}{2W}\cdot\frac{dC}{d\alpha}\cdot\Delta\alpha, \tag{10}$$

where $C$ is the compliance (load point displacement per unit of applied load) of the specimen. The necessary energy for crack extension is

$$\Delta \bar{W} = G_{Ic} b \cdot \Delta a = \frac{K_{Ic}^2}{E'} b \cdot \Delta a, \tag{11}$$

where $E' = E$ for plane stress and $E' = E/(1-\nu^2)$ for plane strain. During crack extension $\Delta U = \Delta \bar{W}$, and

$$K_{Ic} = P\left[\frac{\frac{dC}{d\alpha} \cdot E'}{2Wb}\right]^{1/2} = \frac{P}{B\sqrt{W}}\left[\frac{1}{2}\frac{dC^1}{d\alpha}\frac{\alpha_1 - \alpha_0}{\alpha - \alpha_0}\right]^{1/2} = \frac{P}{B\sqrt{W}} \cdot Y^*, \tag{12}$$

with

$$Y^* = \left[\frac{1}{2}\frac{dC^1}{d\alpha}\frac{\alpha_1 - \alpha_0}{\alpha - \alpha_0}\right]^{1/2}. \tag{13}$$

$C^1 = E'BC$ is the dimensionless compliance. Maximum load occurs at the minimum of the term in brackets.

There exists no analytical solution for the compliance of the short bar specimen. As a first approximation, it can be assumed that $dC^1/d\alpha$ for the chevron notch is identical to that for a straight-through crack. For the straight-through crack, $dC^1/d\alpha$ and $Y$ are related by

$$\frac{dC^1}{d\alpha} = 2Y^2, \tag{14}$$

leading to

$$K_{Ic} = \frac{P}{B\sqrt{W}} Y\left[\frac{\alpha_1 - \alpha_0}{\alpha - \alpha_0}\right]^{1/2} = \frac{P}{B\sqrt{W}} Y^*, \tag{15}$$

with

$$Y^* = Y\left[\frac{\alpha_1 - \alpha_0}{\alpha - \alpha_0}\right]^{1/2}. \tag{16}$$

In Fig. 2, $Y^*$ is plotted against $\alpha$ for a specimen with $W/H = 3$, $\alpha_1 = 1$ and $0 \leq \alpha_0 \leq$

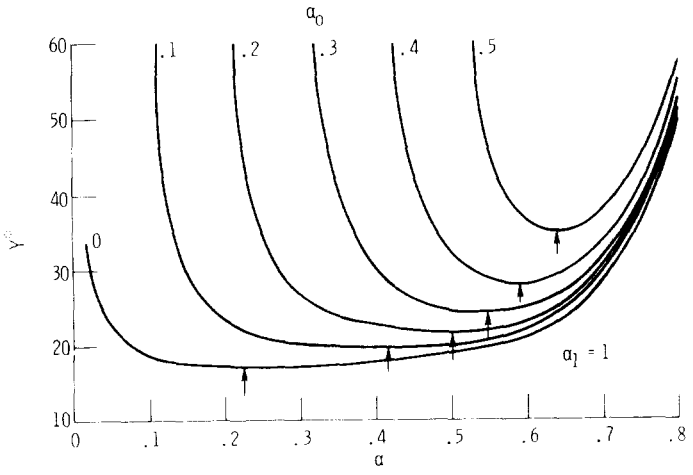


Figure 2. Effect of crack length-to-width ratio $\alpha$ on the analytical dimensionless parameter $Y^*$ for chevron notch specimens of $W/H = 3$ and various $\alpha_0$. The arrows indicate the minimum values of $Y^*$.

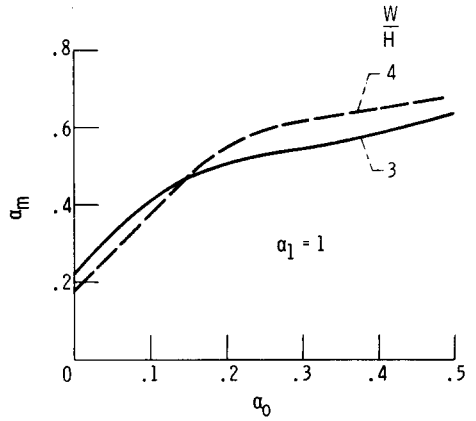


Figure 3. Change in $\alpha_m$ at the minimum value of $Y^*$ with increasing $\alpha_0$.

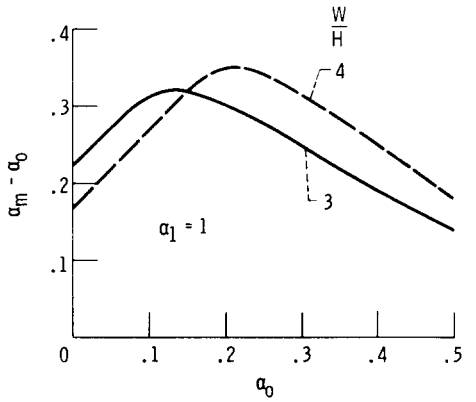


Figure 4. Amount of crack extension ($\alpha_m - \alpha_0$) at the minimum value of $Y^*$ for various $\alpha_0$.

0.5. $Y^*$ has a minimum value $Y_m^*$ (indicated by vertical arrows) that increases and becomes sharper with increasing $\alpha_0$. The maximum load in a fracture mechanics test occurs at this minimum. The crack length-to-width ratio $\alpha_m$ at the minimum $Y_m^*$ of $Y^*$, increases with increasing $\alpha_0$. In Fig. 3, $\alpha_m$ is plotted against $\alpha_0$ for $W/H = 3$ and 4 and $\alpha_1 = 1$. The amount of crack extension to maximum load ($\alpha_m - \alpha_0$) is plotted against $\alpha_0$ in Fig. 4, which shows ($\alpha_m - \alpha_0$) going through a maximum value which is dependent on $W/H$.

## 4. Compliance measurements

### *Experimental procedure*

Compliance specimens (Fig. 5) with $L$–$T$ crack plane orientation were machined from a single 52 mm-thick plate of the aluminum alloy 7075-T651. Specimen cross section was square, with thickness $B$ and height $2H$ equal to 50.8 mm. A 17.8 mm slot was machined 6.4 mm deep into the specimen front face to accommodate loading knife edges. With the specimen positioned firmly against the loading fixture (see Fig. 6) the knife edges contact the specimen on a line 5.1 mm from the front face. The distance from the knife edge contact (loading) line to the specimen back face is the specimen

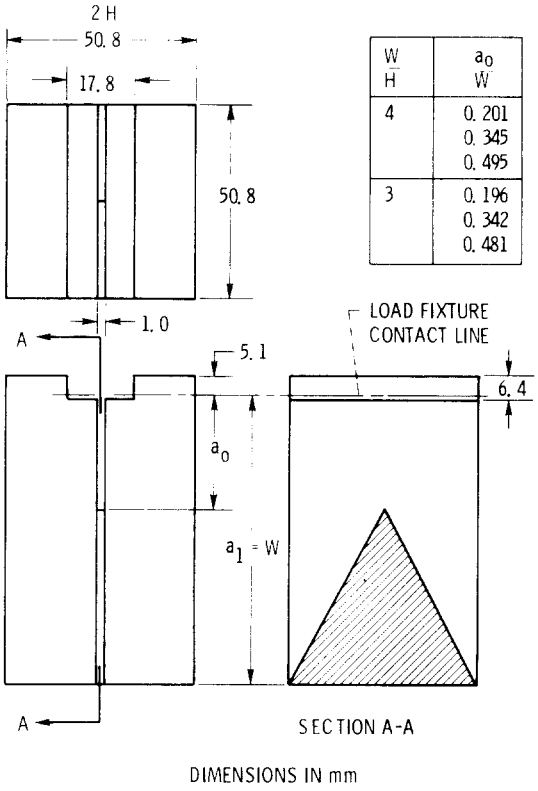


| W/H | $a_0$/W |
|---|---|
| 4 | 0. 201<br>0. 345<br>0. 495 |
| 3 | 0. 196<br>0. 342<br>0. 481 |

Figure 5. Compliance specimens.

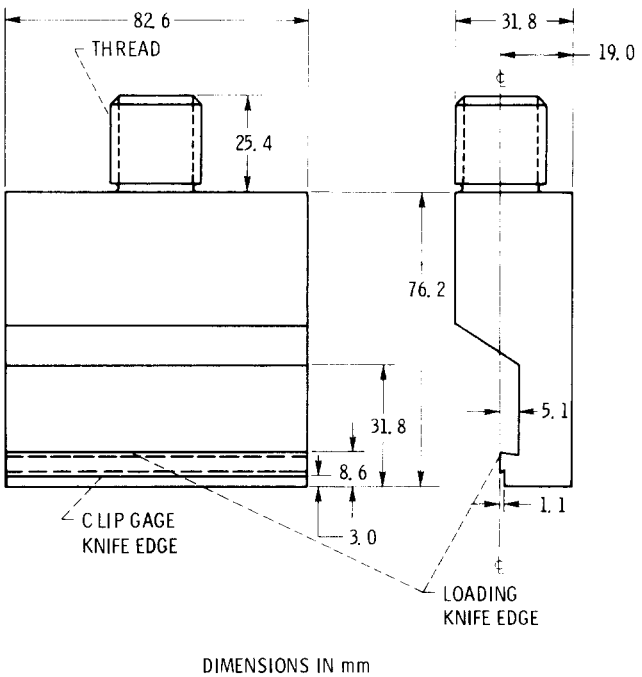


Figure 6. Loading fixture.

width $W$, equal to either 76.2 mm or 101.6 mm (corresponding to $W/H = 3$ and 4, respectively).

Loading fixture knife edge alignment was ascertained by sensing separation of the loading knife edges at outboard locations with two ASTM E-399 clip-in displacement gages, mounted in the clip gage knife edges (see Figs. 6 and 7). When necessary, alignment was adjusted by shimming the fixture. After alignment, nearly the same load *vs.* displacement curve was measured with both clip gages; however, both load *vs.* displacement curves were nonlinear at the beginning of loading. The same nonlinearity was measured when a modified clip gage was placed across the loading knife edges of the loading fixture. This clip gage was operated in tension instead of compression as for the prior installation. The nonlinearity was a result of specimen deformation produced by the knife edges bearing on the specimen. Linear load *vs.* displacement curves were obtained when the displacement was measured directly on the specimen. This was accomplished by using a clip gage having hardened steel cones on the inner surfaces of the gage arms. The cones of the gage, shown in Fig. 7, were set into pairs of small indentations in the top and bottom surfaces of the specimen. Three pairs of indentations were in a single plane which contained the fixture loading knife edges (5.1 mm from the front surface): one pair at mid-thickness and the others near the edge.

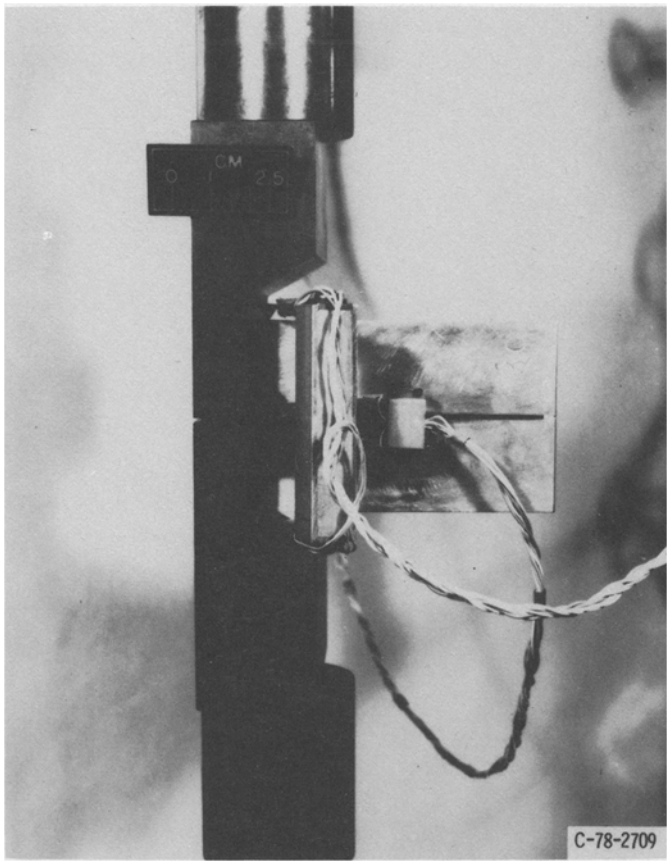


Figure 7. Loading fixture and specimen with attached displacement gages used in complaince measurements.

The crack was simulated by a 0.6 mm saw slot, which was extended incrementally during calibration. For specimens with a straight-through crack, the saw slot was positioned within ±0.25 mm. For specimens with a chevron notch, the saw slot was centered within the 1 mm wide premachined slot. The crack length was measured on both side surfaces. The difference between the two measurements was always less than 0.25 mm.

For each crack length, displacement measurements were made as a function of load in a separate run for each of the three different gage locations. Between each run the specimen was removed from the fixture to reposition the clip gage. The maximum difference in the slope of the load-displacement curves between the three runs was 5% for small crack lengths and <2% for $\alpha > 0.5$. Small changes in the fixture alignment changed the slope measured at the different gage locations. The average of the three slopes however, varied by ±0.3% maximum. A duplicate specimen was tested for one geometry. The agreement between these duplicate specimens was within ±0.5%.

To calculate the dimensionless quantity $C^1 = E'BC$, determination of Young's modulus, $E$, for the alloy 7075-T651 was necessary. Tensile specimens with a test diameter of 12.8 mm were cut from the plate with the tensile axis in the $L$-direction. Some of the specimens were cut from the center of the plate, some from the surface region. Two strain gages were mounted diametrically opposite each other at specimen mid-length. The specimens were loaded in 4 different positions in the testing machine, obtained by a stepwise 90° rotation of the specimen. From the average of all load-displacement readings a value of $E = 6.78 \times 10^4$ N/mm$^2$ was obtained.

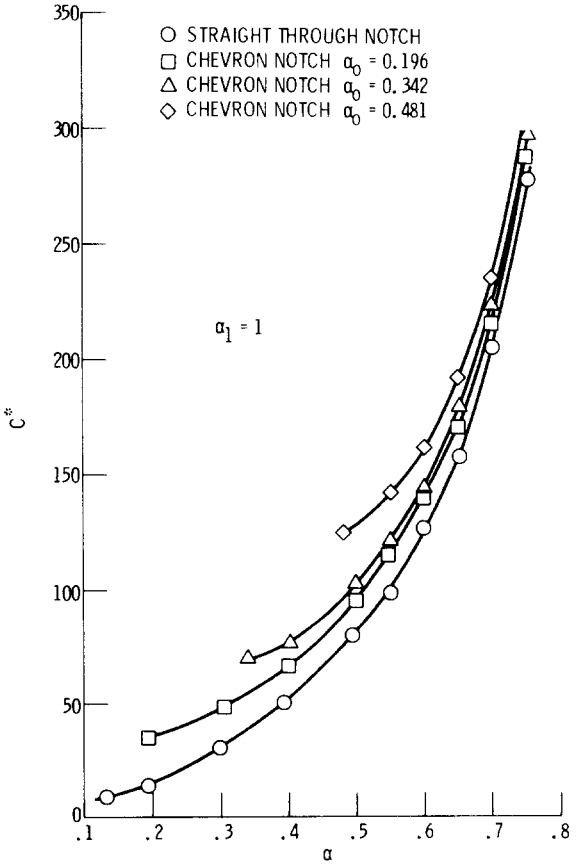


Figure 8. Effect of $\alpha$ on dimensionless compliance for specimens of different initial crack lengths with straight-through and chevron notches for $W/H = 3$.

*Specimens with a straight-through crack*

In Figs. 8 and 9 the dimensionless compliance $C^1 = E'BC$ is plotted against $\alpha$. There is some uncertainty about the usage of the plane strain or plane stress relation when stress intensity factors are derived from compliance measurements [11]. Whereas there is plane strain in the immediate vicinity of the notch at mid-thickness, the bulk of the specimen is nearer the plane stress state. Therefore, Brown and Srawley [12] proposed to omit the $(1 - \nu^2)$ term for $E'$.

To compare the experimental compliance results for a straight-through crack with the calculations of Srawley and Gross [5], $C^1$ was calculated by integration of Eqn. (14), leading to

$$C^1 = 2\int_0^\alpha Y^2 \, d\alpha, \tag{17}$$

with $Y$ from (8). In this calculation $C^1$ for $\alpha = 0$, the compliance of a specimen without a crack, is neglected, leading to slight underestimation of the real compliance. To better compare the experimental results and (17), $C^1(1-\alpha)^2$ instead of $C^1$ is plotted against $\alpha$ in Fig. 10. There is good agreement, the difference between the calculated and experimental results being less than 3% for $\alpha$ between 0.3 and 0.75. More recent calculations of the compliance by Gross [10] have shown even better agreement with the experimental results, especially for small and large values of $\alpha$.

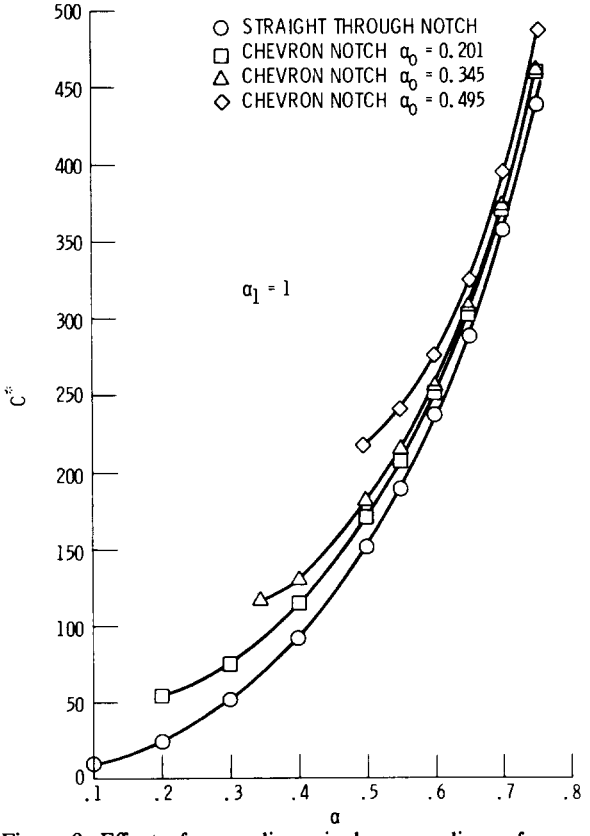


Figure 9. Effect of $\alpha$ on dimensionless compliance for specimens of different initial crack lengths with straight-through and chevron notches for $W/H = 4$.

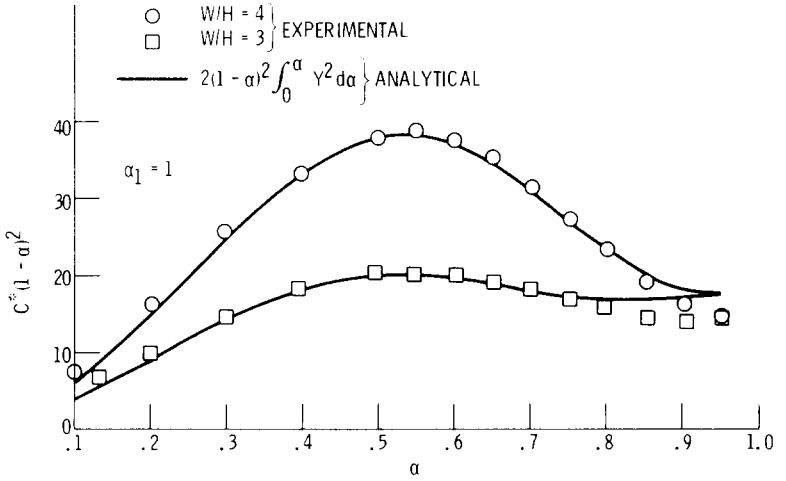


Figure 10. Comparison of experimental and analytical compliance for specimens with straight-through crack.

*Specimens with chevron notches*

From Figs. 8 and 9 it can be seen that the compliance for the specimens with a chevron notch is larger than for specimens with a straight-through crack. With increasing crack length the relative difference decreases.

Fourth degree polynomials were fitted to the logarithms of the $C^1$ data points in the range of $\alpha_0 < \alpha < 0.8$. From these $Y^*$ values were obtained using Eqn. (13). In Figs. 11 and 12, these values are plotted together with $Y^*$ calculated from the analytical approach using Eqns. (8) and (16). For small crack lengths $Y^*$ from the compliance measurements is below $Y^*$ from the calculations, for which a straight-

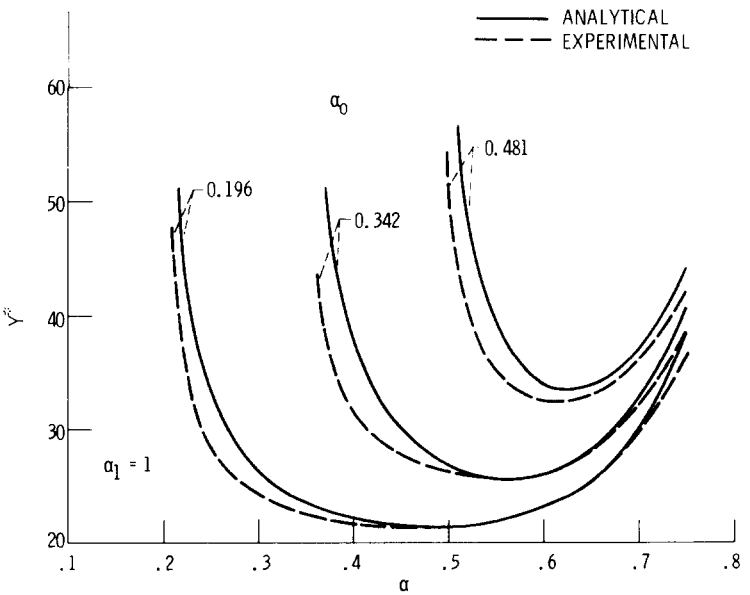


Figure 11. Comparison of experimental and analytical $Y^*$ values for chevron notch specimens of $W/H = 3$ and $\alpha_1 = 1$.

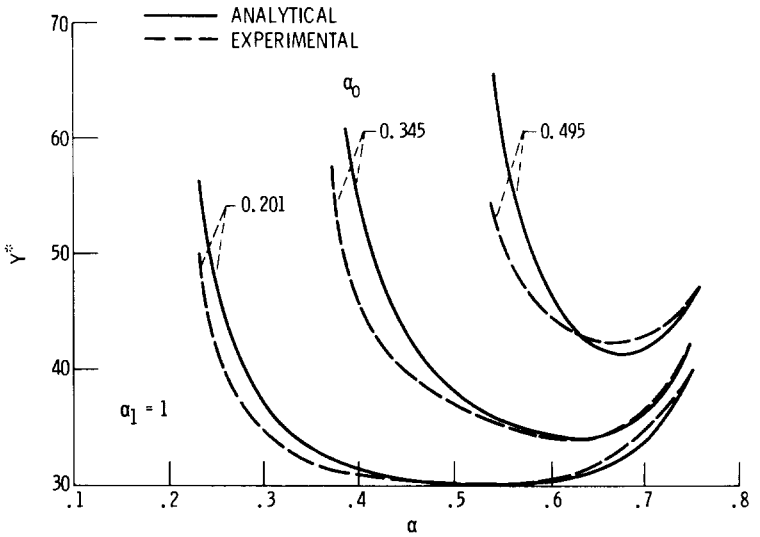


Figure 12. Comparison of experimental and analytical $Y^*$ values for chevron notch specimens of $W/H = 4$ and $\alpha_1 = 1$.

TABLE 1
*Comparison of analytically and experimentally derived values of $Y_m^*$ and the corresponding $\alpha_m$*

| | | Analytical | | Compliance | | Difference in $Y_m^*$, |
|---|---|---|---|---|---|---|
| $W/H$ | $\alpha_0$ | $Y_m^*$ | $\alpha_m$ | $Y_m^*$ | $\alpha_m$ | % |
| 3 | 0.196 | 21.50 | 0.499 | 21.40 | 0.475 | 0.4 |
| | 0.342 | 25.70 | 0.564 | 25.95 | 0.555 | 1.0 |
| | 0.481 | 33.56 | 0.626 | 32.54 | 0.612 | 3.0 |
| 4 | 0.201 | 30.21 | 0.550 | 29.99 | 0.512 | 0.9 |
| | 0.345 | 34.14 | 0.631 | 34.14 | 0.615 | 0 |
| | 0.495 | 41.48 | 0.680 | 42.93 | 0.653 | 3.5 |

through crack was assumed for the compliance. Both $Y^*$ values merge, however, at higher crack lengths. Both $Y^*$ functions have about the same minimum values of $Y_m^*$. In Table 1, $Y_m^*$ is compared for the complaince measurements and the analytical approach. For the specimens with an $\alpha_0$ of about 0.2 and 0.35, the difference between both values is less than 1%. For the $\alpha_0$ values of approximately 0.5 the differences are 3 and 3.5%.

## 5. Discussion

The analytical results and the compliance measurements have shown that $Y^*$ has a minimum for all initial crack lengths $a_0$ investigated. Therefore, fracture toughness can be determined with the short bar specimen by measuring only the maximum load without measurement of crack length. At the maximum load the crack has extended from the tip of the triangular notch to a critical material-independent crack length. This statement is only true when the material has a flat crack growth resistance curve; i.e., the stress intensity factor for a specimen with a straight-through crack is independent of crack extension. This seems to be true for most brittle non-metallic

materials. Only Hüber and Jillek [13] and Bansal and Duckworth [14] found an increase of $K$ with increasing crack extension for some $Al_2O_3$ materials, due probably to crack branching. For metals, a rising crack growth resistance curve is more common [15].

The comparison of the $Y_m^*$ given in Table 1 shows that the analytical approach leading to Eqn. (15) is in very good agreement with the results of the compliance measurements. There are two critical features of the analytical approach: (1) The curve fitting of the boundary collocation results of Srawley and Gross [5] by Eqns. (2) to (8) for the straight-through crack; (2) The assumption that the derivative of the compliance for specimens with a straight-through crack is an adequate approximation for the specimens with a triangular notch.

In Fig. 10 it was shown that there is good agreement between the calculated $C'$ values using Eqn. (17) and the measured compliance. Therefore, (8) is a good description of the behavior for a straight-through crack.

The crack shape of the specimen with a chevron prenotch after some crack extension has the trapezoidal form shown in Fig. 13. The crack is longer at the surface than at the center. Specimen compliance for the trapezoidal crack will exceed that for a straight-through crack. The effect of the surface region diminishes with increasing crack length. This can be seen from the results in Figs. 8 and 9.

At present, there exists no analytical solution for the compliance of a trapezoidal-crack specimen. Bluhm [6, 7], however, has developed a quasi-analytical procedure for handling the non-straight crack front. His functional relationship includes a constant $k$ which has to be determined by comparison of the experimental and analytical results.

The method of Bluhm can be explained using the nomenclature shown in Fig. 13. The specimen is divided into a number of different slices of thickness $\Delta z$.

The compliance of a slice with crack length $x$ is given by

$$C_s = C(\xi) \cdot \frac{B}{\Delta z} \tag{18}$$

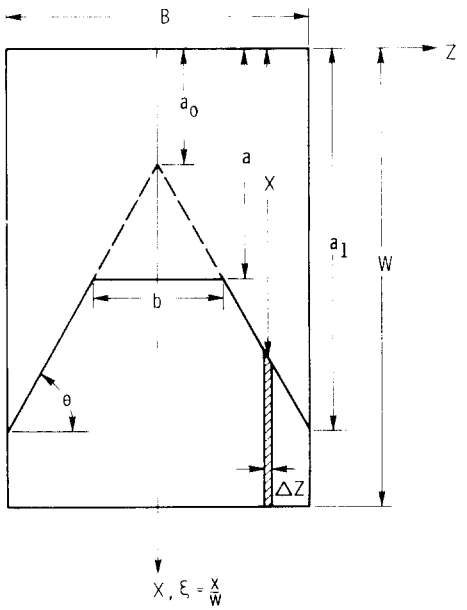


Figure 13. Fracture plane of a specimen with a chevron notch showing the notations used in Bluhm's analysis.

where $C(\xi)$ is the compliance of a straight-through crack specimen of thickness $B$ and crack length-to-width ratio $\xi = x/W$. As a first approximation, the compliance $C_{tr}$ of the total specimen with the trapezoidal crack is given by the sum of the reciprocals of the compliance of all the slices:

$$\frac{1}{C_{tr}} = \sum_{i=1}^{n} \left(\frac{1}{C_s}\right)_i \tag{19}$$

where $n$ is the number of slices. Equation (19) can be written using an integral instead of a summation and taking into account the constant crack front length $b$ in the center of the specimen as

$$\frac{1}{C_{tr}} = \frac{b}{B}\frac{1}{C(\alpha)} + \frac{2}{B}\int_{b/2}^{B/2} \frac{1}{C(\xi)}\,dz \tag{20}$$

where $C(\alpha)$ is the compliance of a straight-through crack specimen of thickness $B$ and crack length-to-width ratio $\alpha = a/W$. If the integration is taken along $\xi$ instead of $z$ and $b/B$ is written in terms of $\alpha$, $\alpha_0$, and $\alpha_1$, using (9); then

$$\frac{1}{C_{tr}} = \frac{\alpha - \alpha_0}{\alpha_1 - \alpha_0}\frac{1}{C(\alpha)} + \frac{1}{\alpha_1 - \alpha_0}\int_{\alpha}^{\alpha_1} \frac{1}{C(\xi)}\,d\xi \tag{21}$$

The compliance of the slices in the section between the edge ($z = \pm B/2$) and the straight-through part ($z = \pm b/2$) of the trapezoidal crack, however, is influenced by interlaminar shear stresses. These interlaminar shear stresses decrease the compliance of the slices. To take this effect into account, Bluhm [6, 7] replaced the thickness of the slice $\Delta z$ by a fictitious thickness $\Delta z'$, given by

$$\Delta z' = k \cdot \Delta z \tag{22}$$

where $k \geq 1$. Thus Eqn. (21) has to be replaced by

$$\frac{1}{C_{tr}} = \frac{\alpha - \alpha_0}{\alpha_1 - \alpha_0}\frac{1}{C(\alpha)} + \frac{k}{\alpha - \alpha_0}\int_{\alpha}^{\alpha_1} \frac{1}{C(\xi)}\,d\xi \tag{23}$$

The shear transfer coefficient $k$ is dependent on the angle $\theta$ of the triangular notch and possibly on $\alpha_1$, and should decrease with increasing $\theta$ or decreasing $\alpha_0$.

To determine $k$ for the short bar specimen, the compliance $C'_{tr} = EBC_{tr}$ was calculated for each investigated geometry for different $k$ factors using Eqn. (23). $C'(\xi) = EBC(\xi)$ was obtained from (17). The calculated compliance was then compared with the experimental results and $k$ determined for the best agreement between experimental and calculated compliance. As an example, results for the specimen with $W/H = 4$ and $\alpha_0 = 0.345$ are shown in Fig. 14. The $k$ coefficients thus determined are plotted in Fig. 15 as a function of $\theta$, along with results of Bluhm [7] for bend specimens. For the investigated short bar specimens, $k$ is larger than for the bend specimens. This can be due to the different specimen geometries or to the larger $\theta$. Comparing $k$ for $W/H = 3$ and $W/H = 4$, it seems that for a given $\alpha_0$, $k$ is independent of $\theta$. However, more measurements are necessary with smaller $\theta$ or larger $\alpha_0$, respectively, to find out the exact relation between $k$, $\theta$, and $\alpha_0$. For this investigation the relation

$$k = -1.38\alpha_0 + 2.67 \tag{24}$$

for $0.2 < \alpha_0 < 0.5$ and $3 < W/H < 4$ and $\alpha_1 = 1$ was obtained.

For the determination of fracture toughness from the maximum load, it is not necessary to use the slice model of Bluhm to obtain the $K_{Ic} - P_{max}$ relation. $Y^*_m$ can be

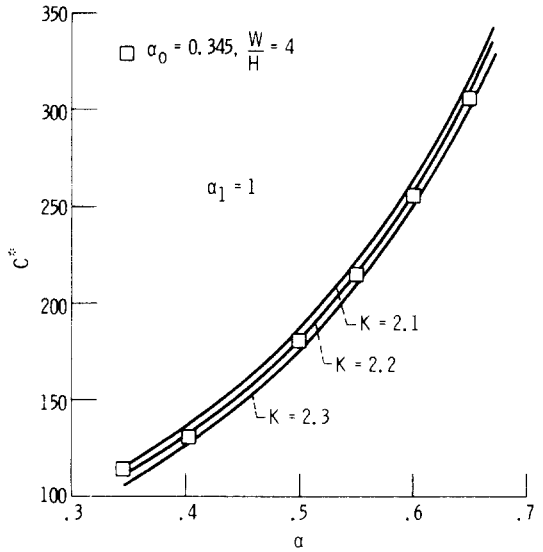


Figure 14. Comparison of the dimensionless compliance between experimental results and calculations using Bluhm's approach with different $k$ values.

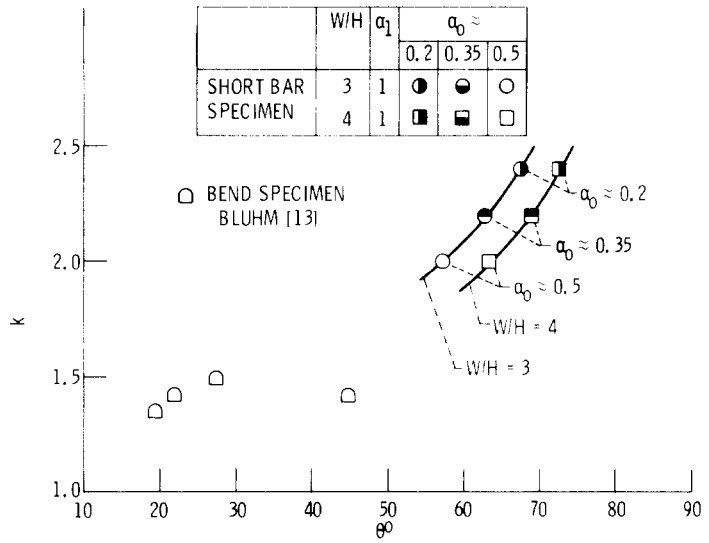


Figure 15. $k$ values as a function of chevron notch angle $\theta$.

calculated from Eqn. (16). To facilitate determining the minimum of $Y^*$ for each investigated specimen geometry, it is desirable to have a function $Y_m^*$ of $\alpha_0$, $W/H$, and $\alpha_1$. For this purpose $Y_m^*$ was calculated for $W/H = 3$, 3.5 and 4, $\alpha_0 = 0.2$, 0.3 and 0.4, and $\alpha_1 = 1$. Then polynomial expressions were fitted through the $Y_m^*$ values, leading to:

$$Y_m^* = 4.08 + 3.95\,W/H + 0.50(W/H)^2 + [-23.15 + 1.15\,W/H + 1.30(W/H)^2]\alpha_0 + [172.5 - 43.5\,W/H + 3.0(W/H)^2]\alpha_0^2. \quad (25)$$

This equation is in agreement with the analytical $Y_m^*$ from (16) within ±0.3% for

$3 < W/H < 4$, $0.2 < \alpha_0 < 0.5$ and $\alpha_1 = 1$. For $\alpha_1 < 1$, Eqn. (25) has to be multiplied by $[(\alpha_1 - \alpha_0)/(1 - \alpha_0)]^{1/2}$.

For some purposes, it is necessary to calculate the stress intensity factor at a load below $P_{max}$ and the corresponding crack length. In those cases the experimental value of $Y^*$ shown in Figs. 11 and 12 have to be used. For specimen geometries different from those of Figs. 11 and 12, but within their bounding range, the compliance can be calculated with Bluhm's model using Eqn. (23) with $k$ obtained from (24). Then $Y^*$ can be calculated from (13).

## 6. Conclusions

The plane-strain fracture toughness, $K_{Ic}$, of brittle materials can be obtained using a short bar specimen with a chevron notch. The advantage of this specimen type is that a sharp natural crack is produced during loading. The load reaches a maximum at a constant material-independent crack length-to-width ratio for a specific geometry. The dimensionless quantity $Y^*$ used in computing $K_{Ic}$ was derived from the superposition of ligament-dependent and ligament-independent solutions for a straight-through crack, and also from experimental compliance calibrations. For materials with a flat crack growth resistance curve, $Y^*$ will have a minimum value $Y_m^*$ at maximum load. The analytical and experimental measurements have shown the following:

1. The experimental compliance measurements for a straight-through notch were within 3% of the analytically derived complaince for crack length-to-width ratios between 0.3 and 0.5.

2. The $Y_m^*$ values obtained from the assumption that the change in compliance with crack extension is the same for a chevron notch as a straight-through notch were within 3.5% of the $Y_m^*$ values obtained from the experimental compliance.

3. The above assumption should not be used to determine $Y^*$ values other than $Y_m^*$ since the agreement with experimental results is poor, particularly at smaller crack length to width ratios.

4. The slice model of Bluhm can be used to obtain $Y^*$. An expression for Bluhm's shear transfer coefficient was developed from the experimental compliance results for the range of specimen geometries investigated.

5. An expression has been given for computing $Y_m^*$ for the short bar specimen with initial crack length-to-width ratios between 0.2 and 0.5, and width-to-half height ratios between 3 and 4.

## Symbols

$a$ crack length
$a_0$ initial crack length (to tip of the chevron notch)
$a_1$ length of chevron notch at the surface
$a_m$ crack length at minimum of $Y^*$
$\Delta a$ crack extension
$b$ length of the crack front
$B$ specimen thickness
$C$ compliance
$C^1$ $= E'BC$
$C_S$ compliance of a slice in Bluhm's model
$C(\alpha)$ compliance of straight-through crack specimen of thickness $B$ and crack length-to-width ratio $\alpha = a/W$.
$C(\xi)$ compliance of straight-through crack specimen of thickness $B$ and crack length-to-width ratio $\xi = x/W$.
$C_{tr}$ compliance of a trapezoidal crack

$E$ Young's modulus
$E'$ $= E$ for plane stress, $= E/(1-\nu^2)$ for plane strain
$G_{Ic}$ critical crack extension force for plane strain
$H$ half of specimen height
$k$ shear transfer coefficient in Bluhm's model
$K_{Ic}$ plane-strain fracture toughness
$P$ load
$P_{max}$ maximum load
$W$ specimen width
$x$ crack length of a slice in Bluhm's model
$Y$ $= KB\sqrt{W}/P$ for a straight-through crack
$Y^*$ $= KB\sqrt{W}/P$ for a trapezoidal crack
$Y_m^*$ minimum of $Y^*$
$\Delta z$ thickness of a slice in Bluhm's model
$\alpha$ $= a/W$
$\xi$ $= x/W$
$\nu$ Poisson's ratio
$\theta$ angle of chevron notch (see Fig. 13)

## REFERENCES

[1] L.M. Barker, *Engineering Fracture Mechanics*, 9 (1977) 361–369.
[2] J. Nakajama, *Journal of the American Ceramic Society*, 48 (1965) 583–587.
[3] H.G. Tattersall and G. Tappin, *Journal of Materials Science*, 1 (1966) 296–301.
[4] L.M. Barker, Eleventh National Symposium on Fracture Mechanics, Blacksburg, Virginia, June 12–14, 1978. (To be published in ASTM-STP-678, 1979.)
[5] J.E. Srawley and B. Gross, *Materials Research and Standards*, 7 (1967) 155–162.
[6] J.I. Bluhm, *Engineering Fracture Mechanics*, 7 (1975) 593–604.
[7] J.I. Bluhm, *Fracture* 1977: *Advances in Research on the Strength and Fracture of Materials, Fourth Inter. Conf. on Fracture*, Vol. 3, D.M.R. Taplin, ed., Pergamon Press, New York (1978) 409–417.
[8] P.C. Paris and G.C. Sih, *Fracture Toughness Testing and its Applications*, ASTM-STP-381, American Society for Testing Materials, Philadelphia (1965) 30–81.
[9] B. Gross and J.E. Srawley, "Stress Intensity Factors by Boundary Collocation for Single-Edge-Notch Specimens Subject to Splitting Forces," NASA TN D-3295 (1966).
[10] B. Gross, private communication.
[11] R.T. Bubsey, D.M. Fisher, M.H. Jones and J.E. Srawley, in *Experimental Techniques in Fracture Mechanics*, Society for Experimental Stress Analysis Monograph 1, A.S. Kobayashi, ed., Iowa State University Press and Society for Experimental Stress Analysis, Cambridge (1973) 76–95.
[12] W.F. Brown, Jr. and J.E. Srawley, *Plane Strain Crack Toughness Testing of High Strength Metallic Materials*, ASTM STP 410, American Society for Testing and Materials, Philadelphia (1966).
[13] H. Hübner and W. Jillek, *Journal of Materials Science*, 12 (1977) 117–125.
[14] G. Bansal and W. Duckworth, *Journal of Materials Science*, 13 (1978) 215–216.
[15] D. Munz, *Elastic-Plastic Fracture Mechanics*, ASTM-STP-668 (1979).

## RÉSUMÉ

Pour déterminer la tenacité à la rupture dans le cas particulier de matériaux fragiles, une éprouvette en forme de barreau court avec section droite rectangulaire et entaille à chevron peut être utilisée. Lorsque la fissure se propage à partir de l'extrémité de l'entaille triangulaire, la charge s'accroît jusqu'à un maximum et ensuite décroît. Pour obtenir la relation entre la tenacité à la rupture $K_{Ic}$ et la charge maximum $P_{max}$, les calculs de Srawley et Gross pour des éprouvettes comportant une fissure droite traversante ont été appliqués aux éprouvettes comportant des entailles en chevron. Pour les éprouvettes à entailles droites traversantes, une expression analytique a été obtenue.

Cette expression a été utilisée pour le calcul de la relation de $K_{Ic} - P_{max}$ sous l'hypothèse que le changement de compliance avec une longueur de fissure correspondant à l'éprouvette à entailles en chevron est la même que dans le cas d'une éprouvette comportant une fissure droite traversante.

Des calibrages comparatifs de la compliance à l'aide d'éprouvettes de géométries différentes se sont montrés en très bon accord avec les résultats analytiques correspondant à la relation $K_{Ic} - P_{max}$. Pour la première partie de l'extension de la fissure avant d'atteindre la charge maximum, la quantité sans dimension $Y^* = K_{Ic}B\sqrt{W}/P$ où $B$ et $W$ sont respectivement l'épaisseur et la largeur de l'éprouvette, et $P$ la charge appliquée, est supérieure dans le cas de l'approche analytique à la valeur obtenue lors des résultats expérimentaux. Cette différence peut être expliquée en appliquant le modèle de découpage en tranches proposé par Bluhm.